Characterization of Lanthanum(III) Chromium(V) Tetraoxide by X-Ray Photoelectron Spectroscopy

Hidetaka KONNO, Hiroto TACHIKAWA, Atsushi FURUSAKI and Ryusaburo FURUICHI

Faculty of Engineering, Hokkaido University, Sapporo 060, Japan

Lanthanum(III) chromium(V) tetraoxide, $LaCrO_4$, was synthesized by a thermal decomposition method and characterized by X-ray photoelectron spectroscopy and *ab initio* molecular orbital calculations. The chromium(V) state in $LaCrO_4$ is stable in both air and vacuum. The electron binding energies, E_B, and Auger parameters, α, of Cr(V) and La(III) indicated that the covalency of the Cr–O bonds in CrO_4 tetrahedra is higher than that in CrO_6 octahedra of $LaCrO_3$, and that La(III) in $LaCrO_4$ is more ionic than in $LaCrO_3$. The results of *ab initio* molecular orbital calculations agreed with the measured characteristics, that is, the electrons are flowing from oxygen to Cr(V) and the covalency plays a significant part in the Cr–O bonds. This behavior of the Cr–O bond was considered to contribute to stabilizing CrO_4^{3-} tetrahedra.

Keywords Lanthanum(III) chromium(V) monazite type oxide, lanthanum(III) chromium(III) perovskite type oxide, X-ray photoelectron spectroscopy, *ab initio* molecular orbital calculation

Lanthanum chromium tetraoxide, $LaCrO_4$, is one of a few Cr(V) compounds which are stable and which can be isolated. The compound can be synthesized by thermal decomposition of $La_2(CrO_4)_3$[1] or $LaCr(C_2O_4)_3 \cdot 9H_2O$.[2,3] It has a monoclinic structure, space group $P2_1/n$[3], similar to monazite and is paramagnetic due to a single unpaired electron on Cr(V), which can be characterized by EPR.[2] The X-ray photoelectron spectroscopy, XPS, measurements of the title compound will provide important information on the electronic configuration of Cr(V) or CrO_4^{3-} state that will be useful for understanding chemical properties of Cr(V) species. The X-ray photoelectron spectroscopic data on Cr(V) is only reported with Na_3CrO_4[4] which is less stable and more difficult to handle than $LaCrO_4$. Due to the low stability of the sodium compound, the Cr 2p spectrum is distorted and the reported electron binding energies, E_B, of Cr 3s and Cr 3p are not accurate, with uncertainties of ± 0.5 eV.

We have found that the title compound can be simply formed as a single phase during the synthesis of perovskite structure $LaCrO_3$ from precursors prepared with La(III)–Cr(VI) equimolar mixed solutions and that the compound is stable at 600° C in air for 12 h.[5] In the present work, E_B values of Cr, La, and O including Auger parameters, α, and the valence band spectrum for $LaCrO_4$ were measured, and the characteristics of the chemical bonds between La, Cr, and O are examined. The electron binding energies for $LaCrO_3$ are also reported.

Experimental

The title compound, $LaCrO_4$, was formed by thermal decomposition of a precursor for 1 h at 600° C in air; the precursor was prepared by vacuum condensation of an equimolar solution of $La(CH_3COO)_3$ and CrO_3 at 70° C, followed by preheating at 400° C in air. Details are reported elsewhere.[5] The XRD pattern and EPR spectrum of the formed $LaCrO_4$ coincided with the reported data[2,3] and are shown elsewhere.[5]

The X-ray photoelectron spectroscopic measurements were carried out by a VG Scientific ESCALAB MkII. The samples were embedded in indium foil on a holder or pressed on a nickel mesh welded on a holder. In a vacuum better than 10^{-8} Pa, the samples were irradiated with Al K_α X-ray (15 kV, 10 – 20 mA). The analyzer pass energy was set at 20 eV which gave a 1.20 eV full width at half maximum, FWHM, of the Au $4f_{7/2}$ spectra for a sputter-cleaned gold foil; only in the energy region of O_{KLL} and Cr_{LMM} was the analyzer pass energy set at 50 eV.

In some measurements, the charge up shift of less than 2 eV was observed for $LaCrO_3$, but no peak broadening was observed. The binding energies were calibrated with E_B[Au $4f_{7/2}$]=84.0 eV for gold particles sputter-deposited on the samples: with some samples E_B[C 1s]= 284.6 eV for surface contaminants calibrated by E_B[Au $4f_{7/2}$] was used as a calibrant. The linearity of the energy scale of the spectrometer was confirmed with the Cu 3p, Cu 3s, Cu 2p, and Au 4f peaks. The measurements were repeated at least twice for three samples from different

batches. The X-ray satellites from Al $K_{\alpha 3,4}$ and Al K_{β} were subtracted by the VGS 5250 data system. The binding energies were determined by assuming that symmetrical Gaussian–Lorentzian mixed functions fit each component of the spectra after subtracting the background by the Shirley method.[6] Although this procedure, as pointed out, is only an approximation[7], the estimated E_B values are not affected beyond the limits of experimental error. It is, however, necessary to be aware that peak intesities may be misleading. The kinetic energies of Auger peaks were determined from the maximum counting rate position.

Molecular orbital calculations were carried out for $[CrO_4]^{n-}$ clusters by the *ab initio* restricted open shell Hartree–Fock (ROHF) method.[8,9] The basis sets employed were Huzinaga's (3333/33/3) for the chromium atoms[10] and the (631/31)+diffuse (sp) function (exponent= 0.0845) for the oxygen atoms.[11] Ionization energies were estimated from Koopmans' theorem.[12] The multi-reference single and double excitation configuration interaction (MR-SD-CI) calculation[13] was also used to determine the electronic states of the clusters. All calculations were performed by a HITAC S820 supercomputer at the Institute for Molecular Science (IMS) in Okazaki.

Results and Discussion

Core electron spectra

The binding energy, E_B, data of core electrons are summarized in Table 1 together with the Auger parameters, α.

The $LaCrO_4$ was stable in a vacuum of 10^{-8} Pa, and no spontaneous decomposition of Cr(V) to Cr(III) were observed for 90 h; decomposition is usually seen with Cr(VI) compounds. Figure 1 shows the Cr 2p spectrum for $LaCrO_4$ after 90 h in a spectrometer vacuum; the spectrum for $LaCrO_3$ is also shown. The values of E_B[Cr 2p] and spin orbit splitting for $LaCrO_4$ are in agreement with those for Na_3CrO_4[4] within the limits of experimental error, after correcting by E_B[Au $4f_{7/2}$]= 84.0 eV. Full width at half maximum, FWHM, of Cr $2p_{3/2}$ peak was 2.50±0.12 eV (±1σ) and slightly wider than FWHM~2.3 eV for the Cr(VI) precursor, but much narrower than that for $LaCrO_3$ (*cf.* Fig. 1). The shape of the spectrum for $LaCrO_4$ is similar to that for Cr(VI) compounds, except that weak satellites are present at about 5.5 eV higher E_B position than the main peaks. This feature was not observed with Na_3CrO_4, probably due to poor resolution and distortion of the spectrum.[4] The appearance of the satellites is likely, as Cr(V) species have a $3d^1$ configuration and $LaCrO_4$ has 1.79 BM at 300 K.[2] In the Cr 3s spectrum for $LaCrO_4$, multiplet splitting was not observed (Fig. 2(A)), whereas for $LaCrO_3$ this was 4.0 eV (Fig. 2(B)). Full width at half maximum of the Cr 3s peak for $LaCrO_4$ was 4.70± 0.39 eV (±1σ), around 10% broadened relative to the Cr(VI) precursor, so that the presence of a hidden peak is unlikely. The disappearance of multiplet splitting may be caused by: (1) single unpaired electron in the 3d orbital, and (2) delocalization or coupling. Absent multiplet splitting suggests that the covalency of the Cr–O bond is high in the CrO_4 tetrahedral structure for $LaCrO_4$. This will be discussed in the following section.

Table 1 Electron binding energies, E_B, and kinetic energies of Auger electrons, E_K, in eV

	$LaCrO_4$	$LaCrO_3$
Cr 3p	46.4 (0.07)	43.2 (0.17)
Cr 3s	77.8 (0.30)	74.4 (0.06)
multiplet satellite	none	78.4 (0.28)
Cr $2p_{3/2}$	578.8 (0.21)	576.1 (0.09)
$2p_{1/2}$	588.0 (0.22)	585.8 (0.05)
spin orbital splitting	9.2	9.7
$Cr_{L3M23M45}$[a]	529.6 (0.21)	529.8 (0.14)
α_{Cr}[Cr $2p_{3/2}$+Cr_{LMM}]	1108.4	1105.9
La $4d_{5/2}$	102.2 (0.33)	101.5 (0.15)
$4d_{3/2}$	105.2 (0.33)	104.7 (0.20)
spin orbit splitting	3.0	3.2
La $3d_{5/2}$	834.9 (0.19)	834.2 (0.21)
satellite	838.6 (0.17)	838.0 (0.28)
$3d_{3/2}$	851.8 (0.17)	851.1 (0.15)
satellite	855.5 (0.18)	854.8 (0.06)
spin orbit splitting	16.9	16.9
$La_{M5N45N45}$[a]	622.3 (0.24)	623.0 (0.71)
α_{La}[La $3d_{5/2}$+La_{MNN}]	1457.2	1457.2
O 1s	529.8 (0.29)	529.5 (0.23)
O_{KLL}[a]	512.8 (0.12)	512.9 (0.56)
α_O[O 1s+O_{KLL}]	1042.6	1042.4

a. Kinetic energy. Uncertainties in parentheses are 1σ in eV.

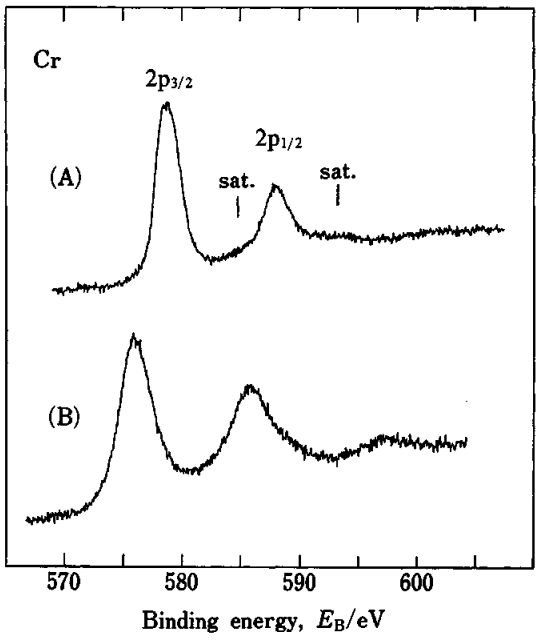

Fig. 1 X-Ray photoelectron spectra of Cr 2p for (A) $LaCrO_4$ and (B) $LaCrO_3$. Satellite peaks are indicated only for $LaCrO_4$.

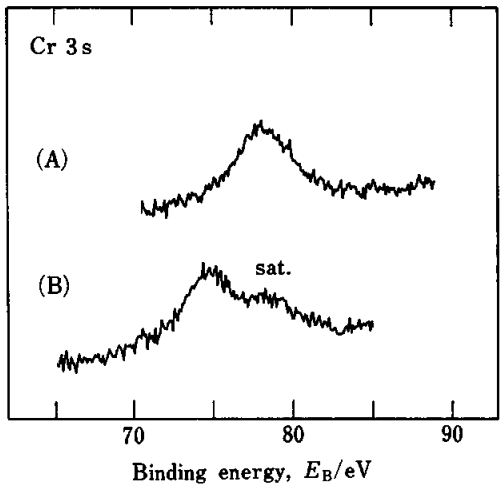

Fig. 2 X-Ray photoelectron spectra of Cr 3s for (A) $LaCrO_4$ and (B) $LaCrO_3$. Sat. indicates a multiplet satellite.

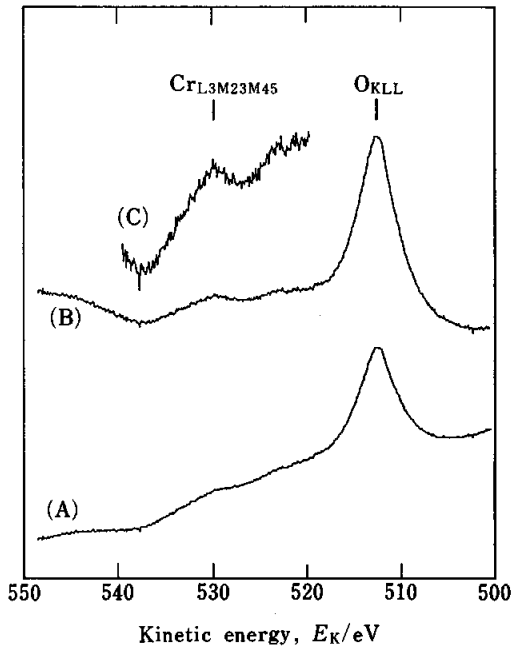

Fig. 3 X-Ray photoelectron spectra of Cr_{LMM} and O_{KLL} region for $LaCrO_4$. (A) original spectrum, (B) (A) after linear background subtraction, and (C) enlarged Cr_{LMM} region of (B).

The peak broadening and the satellites in the Cr 2p spectra for Cr(III) and Cr(IV) compounds are often attributed to the effect of multiplet splitting.[14] Our results, however, suggest that the observed satellites in Cr 2p for $LaCrO_4$ may be due to a shake-up process, as reported for $LaCrO_3$.[15]

The peak position of $Cr_{L3M23M45}$ is often ambiguous under the influence of the $O_{KL23L23}$ peak. Here, in order to make the peak positions distinctive, linear background subtraction was done as shown in Fig. 3. The Auger parameter, $\alpha_{Cr}=E_B[Cr\ 2p_{3/2}]+E_K[Cr_{L3M23M45}]$, for $LaCrO_4$ was 2.5 eV larger than for $LaCrO_3$, due to the differences in $E_B[Cr\ 2p_{3/2}]$ values. The results indicate that the extra-atomic relaxation energy is higher for $LaCrO_4$ than for $LaCrO_3$, and suggests that the electrons are flowing from oxygen to chromium, in agreement with the disappearance of the multiplet splitting.

Both E_B[La] and $E_K[La_{M5N45N45}]$ for $LaCrO_4$ were comparable to those for La_2O_3;[16] the E_B values were about 0.7 eV higher than for $LaCrO_3$ (Table 1). Using La 3d spectra, Berthou *et al.*[17] reported that the covalency of the chemical bond between La(III) and the ligand is proportional to the intensity of the satellite. They reported satellite-to-main-peak intensity ratios for a series of La compounds by peak height, and a I[sat.]/$I[La\ 3d_{5/2}]$ of 0.95 for $LaCrO_3$ and 0.86 for La_2O_3. We also measured the intensity ratio for $LaCrO_3$ both by height and area, but did not obtain such high values. Estimated by area, our ratio for $LaCrO_3$ was below 0.80 and around 0.77 for $LaCrO_4$, depending on the limitations in peak separation. Berthou *et al.* indicated that the covalency to intensity ratio is a much better indicator of the covalent bond than the satellite energy separations, but they did not provide theoretical justification. For the present discussion, it is not appropriate to consider the characteristics of the chemical bond between La(III) and the CrO_4 group based on the intensity ratio.

The lanthanum atom in monoclinic $LaCrO_4$ is asymmetrically surrounded by six CrO_4 tetrahedra (La coordination number=9), whereas that in orthorhombic $LaCrO_3$ is the center of eight CrO_6 octahedra (La coordination number=12). From this structural difference and the differences in E_B for La(III), it is probable that La(III) in $LaCrO_4$ is more ionic than in $LaCrO_3$. The absence of differences between α_{La} values also indicates that the differences in E_B values can be attributed to the initial state effects.

There is some uncertainty in the spin orbit separation of La 4d due to the peak separation. Howng and Thorn[18] reported that La 4d peak can be separated into La $4d_{5/2}$ and La $4d_{3/2}$ each having a satellite. However, they provide neither criteria for separating the peaks nor a method of background subtraction; but their intensity ratio, $I[La\ 4d_{5/2}]/I[La\ 4d_{3/2}]$, after the separation agreed with the theoretical value reported by Burroughs *et al.*[19] This agreement, however, does not verify the correctness of their peak separation, since the total intensity ratio including satellites should be compared. We found that at least one limiting condition is necessary to separate the La 4d peaks; the limiting condition may be the same FWHM for the peak pair, the same Gaussian–Lorentzian mixing ratio, a certain fixed splitting between the main peak and the satellite, or some similar one. Here, the calculations were carried out by using one value of Gaussian–Lorentzian mixing ratio for the main peak pair and another value for the satellite pair. The results where the total intensity ratio including satellites agreed with a calculated cross section ratio[20] were taken as the final values. An example of the results is shown in

Fig. 4.

The values of E_B[Cr 2p] for $LaCrO_3$ are in agreement with those reported by Howng and Thorn[15] after correcting by E_B[Au $4f_{7/2}$]=84.0 eV but other E_B values in Table 1 do not agree with their results. One reason is that they used E_B[C 1s] value for contamination as a reference peak even after ion sputtering: this is not an appropriate, since the E_B[C 1s] value for contamination changes due to ion sputtering. The large differences in measured E_B[Cr 3p], E_B[Cr 3s], E_B[La 4d], and E_B[La 3d] values cannot be explained by this alone. The differences may be explained by the following: (1) there are many misprints and inconsistencies in the values in tables, figures, and text in the papers;[15,19] (2) for Cr_2O_3, the E_B[Cr 2p] values agree with those reported by others[16,21,22], but the E_B[Cr 3s] value is about 1 eV higher than other data;[21,22] and (3) for La_2O_3, the E_B[La 3d] values are about 2 eV lower than data reported elsewhere.[16]

Valence band spectra and calculated electronic states

The valence band for $LaCrO_4$ starts from E_B~7.5 eV, which is about 9.5 eV above La $5p_{3/2}$, and it extends to the Fermi edge, as shown in Fig. 5. There is a low density band just below the Fermi edge; the presence of the low density band is supported by the reproducible shape of the valence band spectrum. The peak positions of La 5p and O 2s are distinguishable without peak separation and no photoemission is observable between these peaks and the valence band, so it is unlikely that there is an interaction between them.

For *ab initio* ROHF-MO calculations[8,9], the following assumptions were made as a first approximation: (1) the calculations are possible with the one unit model, the CrO_4^{3-} cluster, since, as mentioned above, the ionic character of La(III) for $LaCrO_4$ is comparable to that for La_2O_3 (>75%); and (2) the molecular symmetry of the cluster is T_d and the Cr–O bond length is 0.16 nm. The latter was assumed based on the structure of similar monazite type minerals.[23] The accurate atomic arrangement of $LaCrO_4$ is not established, though the X-ray diffraction data has been reported.[3] The absolute energy positions of the calculated molecular orbitals depend on the Cr–O bond length, but, the order of the orbitals from the Fermi edge need not change with the assumed Cr–O bond lengths allowed for this cluster.

The calculated contour maps for singly occupied molecular orbitals of the CrO_4^{3-} cluster are shown in Fig. 6. The maps indicate that the spin orbital is composed of an antibonding $\pi^*(dz^2\text{-}2p)$ orbital which is formed by interaction between Cr(dz^2) and O(2p) orbitals. The electronic configurations in the valence band were calculated to be

$$(3dz^2)^{1.13}(3dx^2\text{-}y^2)^{0.72}(3dxy)^{0.44}(3dyz)^{0.72}(3dzx)^{0.72}(4s)^{0.078}.$$

This means that the population of electrons on the dz^2 orbital of Cr is larger than on other orbitals, indicating that an unpaired electron is occupying the dz^2 orbital.

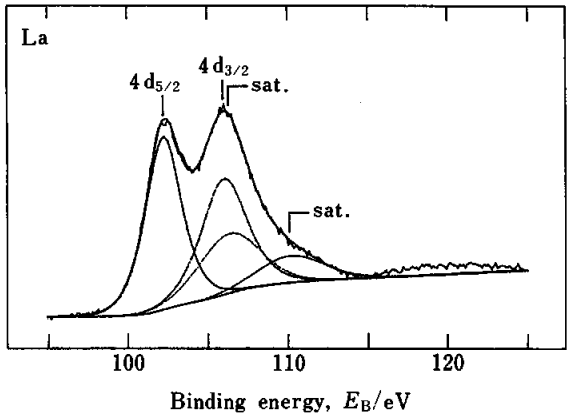

Fig. 4 An example of peak separation of La 4d spectrum for $LaCrO_4$.

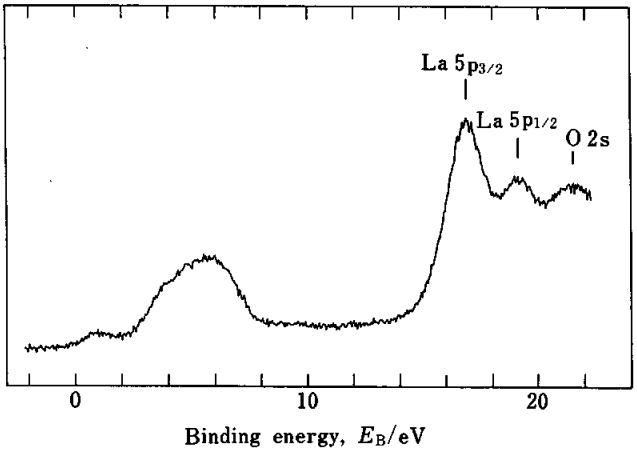

Fig. 5 X-Ray photoelectron spectrum of valence band for $LaCrO_4$.

The atomic charges distributed over the CrO_4^{3-} cluster were calculated to be +2.4 for Cr and −1.3 for O, showing that the charges on O^{2-} are flowing into Cr^{5+}. The overlap charge between Cr ion and O ion is positive, 0.1176. The results indicate that covalency plays a significant role in the Cr–O bonds of the CrO_4 tetrahedral structure in $LaCrO_4$. These features agree with the results of XPS measurements. This behavior of the Cr–O bond was considered to contribute to stabilizing CrO_4^{3-} tetrahedra.

The theoretical ionization energies calculated at the ROHF level were compared with the measured valence band spectrum, as shown in Table 2. Due to the assumptions used in the calculations, the absolute energy values are slightly different from the observed peak positions (*cf.* O 2s), however, it is still possible to assign the measured bands as in the table. It should be noted that the assignment of O 2p non-bonding levels is not certain: they may be present in the weak peak just below the Fermi edge or included in the large peak. If included in the large peak, the weak peak may be assigned

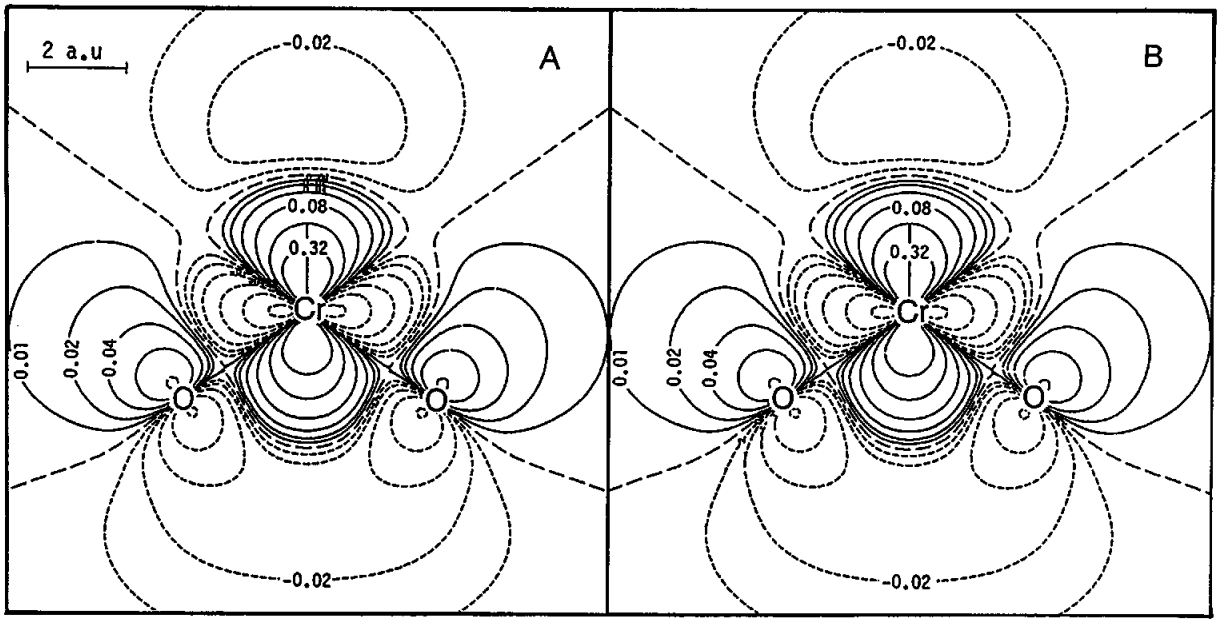

Fig. 6 Molecular orbital contour maps for the spin orbital of CrO_4^{3-} cluster. Solid and broken lines indicate positive and negative amplitudes of wave function. The values are calculated at the ROHF level. (A) XZ plane and (B) YZ plane.

Table 2 Calculated energy levels in the valence band in eV

Calculated values	Experimental peak positions	Assignment
0.99	0.5	O 2p non-bonding (and/or
1.05, 1.05	-2	Cr 3d unpaired electron)
2.41, 2.43, 2.45, 2.45	2.5-7.5	O 2p–Cr 3d bonding[a]
5.18, 5.59, 5.60, 5.66		Cr 3d–O 2p bonding[b]
	16.9	La $5p_{3/2}$
	19.1	La $5p_{1/2}$
22.92, 22.92, 22.92, 23.58	21.4	O 2s

a. Electrons distribute mainly on the oxygen atoms. b. Electrons distribute mainly on the chromium atom.

to a 3d unpaired electron level.

References

1. H. Schwartz, *Z. Anorg. Allge. Chem.*, **322**, 1 (1963).
2. A. Roy and K. Nag, *J. Inorg. Nucl. Chem.*, **40**, 1501 (1978).
3. JCPDS 36-93.
4. L. Lavielle and H. Kessler, *J. Electron Spectrosc. Relat. Phenom.*, **8**, 95 (1976).
5. A. Furusaki, H. Konno and R. Furuichi, *Nippon Kagaku Kaishi*, **1992**, 612.
6. D. A. Shirley, *Phys. Rev.*, **B5**, 4709 (1972).
7. S. Tougaard, *Surf. Interface Anal.*, **11**, 453 (1988).
8. H. Kashiwagi, T. Takada, E. Miyoshi, S. Obara and F. Sasaki, *ab-initio RHF calculation program, JAMOL4* (1988).
9. C. C. J. Roothan, *Rev. Mod. Phys.*, **32**, 179 (1960).
10. "*Physical Science Data*", Vol. 16, ed. S. Huzinaga, Elsevier, Amsterdam, 1984.
11. T. Clark, J. Chandrasekhar, G. W. Spitznagel and P. V. R. Schleyer, *J. Comput. Chem.*, **4**, 294 (1983).
12. T. Koopmans, *Physica*, **1**, 104 (1933).
13. R. J. Buenker and Peyerimhoff, *Theor. Chim. Acta*, **35**, 33 (1974); A. Murakami, H. Iwaki, H. Terashima, T. Shoda, T. Kawaguchi and T. Noro, *MR-SD-CI program, MICA3*, 1985.
14. *e.g.* I. Ikemoto, K. Ishii, S. Kinoshita, H. Kuroda, M. A. Alario Franco and J. M. Thomas, *J. Solid State Chem.*, **17**, 425 (1976).
15. W.-Y. Howng and R. J. Thorn, *J. Phys. Chem. Solids*, **41**, 75 (1980).
16. C. D. Wagner, "*Practical Surface Analysis, 2nd ed.*", eds. M. P. Seah and D. Briggs, pp. 595, 645, John Wiley, New York, 1990.
17. H. Berthou, C. K. Jørgensen and C. Bonnelle, *Chem. Phys. Lett.*, **38**, 199 (1976).
18. W.-Y. Howng and R. J. Thorn, *Chem. Phys. Lett.*, **56**, 463

(1978).
19. P. Burroughs, A. Hamnett, A. F. Orchard and G. Thornton, *J. Chem. Soc. Dalton Trans,* **1976**, 1686.
20. J. H. Scofield, *J. Electron Spectrosc. Relat. Phenom.,* **8**, 129 (1976).
21. K. Asami and K. Hashimoto, *Corr. Sci.,* **17**, 559 (1977).
22. H. Konno, *J. Metal Finish. Soc. Jpn.,* **29**, 425 (1978).
23. R. W. G. Wyckoff, "*Crystal Structures, 2nd ed.*", Vol. 3, Interscience, New York, 1965.

(Received May 18, 1992)
(Accepted June 25, 1992)